Equation of state and chiral transition in soft-wall AdS/QCD with a more realistic gravitational background*

Zhen Fang(房震)[1;1)] Yue-Liang Wu(吴岳良)[2,3;2)]

[1]Department of Applied Physics, School of Physics and Electronics, Hunan University, Changsha 410082, China
[2]CAS Key Laboratory of Theoretical Physics, Institute of Theoretical Physics, Chinese Academy of Sciences, Beijing 100190, China
[3]International Centre for Theoretical Physics Asia-Pacific (ICTP-AP), University of Chinese Academy of Sciences, Beijing 100049, China

Abstract: We construct an improved soft-wall AdS/QCD model with a cubic coupling term of the dilaton and the bulk scalar field. The background fields in this model are solved by the Einstein-dilaton system with a nontrivial dilaton potential, which has been shown to reproduce the equation of state from the lattice QCD with two flavors. The chiral transition behaviors are investigated in the improved soft-wall AdS/QCD model with the solved gravitational background, and the crossover transition can be realized. Our study provides the possibility to address the deconfining and chiral phase transitions simultaneously in the bottom-up holographic framework.

Keywords: AdS/QCD, chiral transition, equation of state

DOI: 10.1088/1674-1137/abab90

1 Introduction

Quantum chromodynamics (QCD) describes the strong interaction between quarks and gluons. Because of asymptotic freedom, the method of perturbative quantum field theory can be applied to study high-energy properties of QCD matter in the ultra-violet (UV) region. However, the strong coupling nature of QCD at low energies makes it impossible to apply the perturbative method for handling nonperturbative problems of QCD. Quark confinement and chiral symmetry breaking are two essential features of low-energy QCD, and the related physics fields have attracted significant interest for many years. The QCD phase transition is such a field that enabled investigation of the low-energy physics of QCD [1]. With increasing temperature, we know that the QCD matters undergo a crossover transition from the hadronic state to the state of quark-gluon plasma (QGP), along with the deconfining process of the partonic degrees of freedom and the restoration of chiral symmetry [2-4].

Numerous nonperturbative methods have been developed to study the QCD phase transition and issues in low-energy hadron physics [5-8]. As a powerful method, lattice QCD is widely used to tackle the low-energy QCD problems from the first principle. However, there are limitations to this method, such as in the case of nonzero chemical potential, arising due to the sign problem. In recent decades, the anti-de Sitter/conformal field theory (AdS/CFT) correspondence has provided a powerful tool for us to study the low-energy physics of QCD by the holographic duality between a weakly coupled gravity theory in asymptotic AdS_5 spacetime and a strongly coupled gauge field theory on the boundary [9-11]. Numerous studies have been conducted in this field, following either the top-down approach or the bottom-up approach [12-62].

Holographic studies in the top-down approach have shown that the simplest nonsupersymmetric deformation of AdS/CFT with nontrivial dilaton profiles is capable of reproducing the confining properties of QCD [63, 64], and realizing the pattern of chiral symmetry breaking with quarks mimicked by the D7-brane probes [65-69]. However, it is not clear how to generate the crossover transition indicated from lattice QCD in the top-down

Received 9 April 2020, Revised 14 June 2020, Published online 11 August 2020

* Supported in part by the National Natural Science Foundation of China (NSFC) (11851302, 11851303, 11690022, 11747601), the Strategic Priority Research Program of the Chinese Academy of Sciences (XDB23030100) as well as the CAS Center for Excellence in Particle Physics (CCEPP). Z. F. is also Supported by the NSFC (11905055) and the Fundamental Research Funds for the Central Universities (531118010198)

1) E-mail: zhenfang@hnu.edu.cn
2) E-mail: ylwu@itp.ac.cn

framework. Indeed, AdS/CFT per se is inadequate to provide a complete description for the thermodynamics of QCD because of its semi-classical character inherited from the type IIB string theory in the low-energy approximation and the large N limit. The string-loop corrections have to be considered to provide an adequate account for thermal QCD. Nevertheless, the qualitative description by such a holographic approach is still meaningful and indeed has provided significant insights in our study of low-energy QCD.

It was shown that the deconfinement in the pure gauge theory corresponds to a Hawking-Page phase transition between a thermal AdS space and a black hole configuration [70-72]. However, numerous studies employing the bottom-up approach indicate that we can use a bulk gravity system with a nontrivial dilaton profile to characterize the equation of state and the deconfining behaviors of QCD [73-90]. Moreover, unlike the holographic studies of pure gauge theory, the crossover transition in these bottom-up models is only related to the black hole solution solved from the Einstein-dilaton(-Maxwell) system, which is contrary to the usual claim that the black hole is dual to the deconfined phase at high temperatures. As we cannot expect to make use of two distinct bulk geometries to generate a smooth crossover transition in AdS/QCD [27], it seems more natural to provide a description of thermal QCD properties only in terms of the black hole solution. However, in this case we must make sure that the black hole is stable when compared with the thermal gas phase.

In the bottom-up approach, the soft-wall AdS/QCD model provides a concise framework to address the issues on chiral transition [18]. However, it has been shown that the original soft-wall model lacks spontaneous chiral symmetry breaking [18, 28]. The chiral transitions in the two-flavor case have been studied in a modified soft-wall AdS/QCD model, where the second-order chiral phase transition in the chiral limit and the crossover transition with finite quark masses are first realized in the holographic framework [91, 92]. In Ref. [93], we proposed an improved soft-wall model, which can generate both the correct chiral transition behaviors and the light meson spectra in a consistent manner. The generalizations to the $2+1$ flavor case have been considered in Refs. [94-96], and the quark-mass phase diagram that is consistent with the standard scenario can be reproduced. The case of finite chemical potential has also been investigated [97-99], and the chiral phase diagram containing a critical end point can be obtained from the improved soft-wall AdS/QCD model with $2+1$ flavors [98, 99].

It should be noted that the AdS-Schwarzschild black-hole background has been used in most of studies of chiral transition at zero chemical potentials. However, such an AdS black-hole solution is dual to a conformal gauge theory, which cannot generate the QCD equation of state without breaking the conformal invariance [73]. As mentioned above, one can resort to the Einstein-dilaton system with a nontrivial dilaton profile to rescue this issue. Hence, we wonder whether the correct chiral transition behaviors can still be obtained from a soft-wall AdS/QCD model with a solved gravitational background from the Einstein-dilaton system. In this work, we shall consider this issue and try to combine the description of chiral transition with that of the equation of state, which signifies deconfinement in a unified holographic framework.

This paper is organized as follows. In Sec. 2, we consider an Einstein-dilaton system with a nontrivial dilaton potential, which can produce the equation of state that is consistent with lattice results in the two-flavor case. The vacuum expectation value (VEV) of the Polyakov loop is computed in such a background system and compared with the lattice data. In Sec. 3, we propose an improved soft-wall AdS/QCD model with a cubic coupling term of the dilaton and the bulk scalar field. The chiral transition behaviors are considered in the two-flavor case. The crossover behaviors of chiral transition can be realized in this model. The parameter dependence of chiral transition is also investigated. In Sec. 4, we present a brief summary of our work and conclude with some remarks.

2 QCD equation of state from holography

2.1 Einstein-dilaton system

In previous studies, we proposed an improved soft-wall AdS/QCD model with a running bulk scalar mass $m_5^2(z)$, which yields an appropriate characterization for the chiral transition in both the two-flavor and the $2+1$ flavor case [93, 96]. However, the AdS-Schwarzschild black hole employed in this model cannot describe the thermodynamical behaviors of the QCD equation of state and other equilibrium quantities, which indicate obvious violation of conformal invariance [73]. To acquire these basic features of thermal QCD, we must construct a proper gravity background other than the AdS-type black hole to break the conformal invariance of the dual gauge theory. The minimal action of such a background system is given in the string frame as

$$S_g = \frac{1}{2\kappa_5^2}\int \mathrm{d}^5x\sqrt{-g}\mathrm{e}^{-2\phi}\left[R+4(\partial\phi)^2-V(\phi)\right], \qquad (1)$$

where $\kappa_5^2 = 8\pi G_5$, and a dilaton field ϕ has been introduced to account for relevant deformations of the dual conformal field theory. The dilaton $\phi(z)$ is assumed to depend only on the radial coordinate z. The key point of this model is to find a particular form of the dilaton potential $V(\phi)$ with necessary ingredients to describe the QCD thermodynamics, such as the equation of state.

The metric of the bulk geometry in the string frame can be written as

$$\mathrm{d}s^2 = \frac{L^2 \mathrm{e}^{2A_S(z)}}{z^2}\left(-f(z)\mathrm{d}t^2 + \mathrm{d}x^i\mathrm{d}x^i + \frac{\mathrm{d}z^2}{f(z)}\right), \tag{2}$$

with the asymptotic structure of AdS_5 spacetime at $z \to 0$ to guarantee the UV conformal behavior of the dual gauge theory on the boundary. We take the AdS radius $L = 1$ for convenience. To simplify the calculation, we work in the Einstein frame with the metric ansatz

$$\mathrm{d}s^2 = \frac{L^2 \mathrm{e}^{2A_E(z)}}{z^2}\left(-f(z)\mathrm{d}t^2 + \mathrm{d}x^i\mathrm{d}x^i + \frac{\mathrm{d}z^2}{f(z)}\right). \tag{3}$$

The warp factors in the two frames are related by $A_S = A_E + \frac{2}{3}\phi$, in terms of which the background action in the Einstein frame can be obtained from the string-frame action (1) as

$$S_g = \frac{1}{2\kappa_5^2}\int \mathrm{d}^5x\sqrt{-g_E}\left[R_E - \frac{4}{3}(\partial\phi)^2 - V_E(\phi)\right], \tag{4}$$

with $V_E(\phi) \equiv \mathrm{e}^{\frac{4\phi}{3}}V(\phi)$ (the subscript E denotes the Einstein frame).

2.2 EOM with a nontrivial dilaton potential

The independent Einstein equations can be derived by the variation of the action (4) with respect to the metric g_{MN},

$$f'' + 3A_E'f' - \frac{3}{z}f' = 0, \tag{5}$$

$$A_E'' + \frac{2}{z}A_E' - A_E'^2 + \frac{4}{9}\phi'^2 = 0. \tag{6}$$

The equation of motion (EOM) of the dilaton ϕ in the Einstein frame can also be derived as

$$\phi'' + \left(3A_E' + \frac{f'}{f} - \frac{3}{z}\right)\phi' - \frac{3\mathrm{e}^{2A_E}\partial_\phi V_E(\phi)}{8z^2 f} = 0. \tag{7}$$

Given the dilaton potential $V_E(\phi)$, the numerical solution of the background fields A_E, f, and ϕ can be solved from the coupled differential equations (5), (6), and (7).

Although there are few constraints on the form of the dilaton potential from the top-down approach of AdS/QCD, it has been shown that a proper $V_E(\phi)$ can be constructed from the bottom up to describe the equation of state of the strongly coupled QGP [73, 74]. Near the boundary, the bulk geometry must approach the AdS_5 spacetime, which corresponds to a UV fixed point of the dual gauge theory. This requires that the dilaton potential at UV has the following asymptotic form:

$$V_c(\phi_c \to 0) \simeq -\frac{12}{L^2} + \frac{1}{2}m^2\phi_c^2 + O(\phi_c^4), \tag{8}$$

with the rescaled dilaton field defined by $\phi_c = \sqrt{\frac{8}{3}}\phi$, in terms of which the action (4) can be recast into the canonical form

$$S_g = \frac{1}{2\kappa_5^2}\int \mathrm{d}^5x\sqrt{-g_E}\left[R_E - \frac{1}{2}(\partial\phi_c)^2 - V_c(\phi_c)\right], \tag{9}$$

with $V_c(\phi_c) = V_E(\phi)$. As argued in Ref. [74], the dilaton potential at IR takes an exponential form $V_c(\phi_c) \sim V_0\mathrm{e}^{\gamma\phi_c}$ with $V_0 < 0$ and $\gamma > 0$ to yield the Chamblin-Reall solution, whose adiabatic generalization links the QCD equation of state to the specific form of $V_c(\phi_c)$.

According to AdS/CFT, the mass squared of ϕ_c is related to the scaling dimension Δ of the dual operator on the boundary by $m^2L^2 = \Delta(\Delta-4)$ [16]. We only consider the case of $2 < \Delta < 4$, which corresponds to the relevant deformations satisfying the Breitenlohner-Freedman (BF) bound [73, 77]. It is usually assumed that the dilaton field ϕ_c is dual to the gauge-invariant dimension-4 glueball operator $\mathrm{tr}\,F_{\mu\nu}^2$, although other possibilities, such as a dimension-2 gluon mass operator, have also been considered [32]. Following Ref. [73], we attempt to match QCD at some intermediate semi-hard scale, where the scaling dimension of $\mathrm{tr}\,F_{\mu\nu}^2$ would have a value smaller than 4. One remark is that the asymptotic freedom cannot be captured in this way, but will be replaced by conformal invariance when above the semi-hard scale [73]. The full consideration might go beyond the supergravity approximation. In this study, we take $\Delta = 3$, which has been shown to describe the equation of state from lattice QCD with $2+1$ flavors [78, 79] and is also easier to implement in the numerical calculation. We note that other values of Δ can also be used to mimick the QCD equation of state, and this is by and large determined by the particular form of the dilaton potential and the specific parameter values [73, 77]. The main aim of our study is to investigate the chiral properties based on a gravitational background, which can reproduce the QCD equation of state. Thus, we did not delve into the possible influence of the value of Δ on the results considered in our work. Following the studies in Ref. [73], we choose a relatively simple dilaton potential, which satisfies the required UV and IR asymptotics,

$$V_c(\phi_c) = \frac{1}{L^2}\left(-12\cosh\gamma\phi_c + b_2\phi_c^2 + b_4\phi_c^4\right), \tag{10}$$

where γ and b_2 are constrained by the UV asymptotic form (8) as

$$b_2 = 6\gamma^2 + \frac{\Delta(\Delta-4)}{2} = 6\gamma^2 - \frac{3}{2}. \tag{11}$$

The dilaton potential $V_E(\phi)$ has the form

$$V_E(\phi) = V_c(\phi_c) = V_c(\sqrt{8/3}\phi). \tag{12}$$

We see that the Einstein-dilaton system given above can also be used to mimick the two-flavor lattice results of the QCD equation of state, whereby the dilaton potential $V_E(\phi)$ and the background geometry can be reconstructed for the two-flavor case.

2.3 Equation of state

Now, we consider the equation of state in the Einstein-dilaton system with the given form of the dilaton potential (10). First, the background geometry has an event horizon at $z=z_h$, which is determined by $f(z_h)=0$. In terms of the metric ansatz (3), the Hawking temperature T of the black hole is given by

$$T=\frac{|f'(z_h)|}{4\pi}, \tag{13}$$

and the entropy density s is related to the area of the horizon,

$$s=\frac{\mathrm{e}^{3A_E(z_h)}}{4G_5z_h^3}. \tag{14}$$

Thus, we can compute the speed of sound c_s by the formula

$$c_s^2=\frac{\mathrm{d}\log T}{\mathrm{d}\log s}. \tag{15}$$

Moreover, the pressure p can be obtained from the thermodynamic relation $s=\dfrac{\partial p}{\partial T}$ as

$$p=-\int_{\infty}^{z_h}s(\bar{z}_h)T'(\bar{z}_h)\mathrm{d}\bar{z}_h. \tag{16}$$

The energy density $\varepsilon=-p+sT$ and the trace anomaly $\varepsilon-3p$ can also be computed. Then, we can study the temperature dependence of the equation of state in such an Einstein-dilaton system. As we constrain ourselves to the two-flavor case, the equation of state from lattice QCD with two flavors is used to construct the dilaton potential $V_E(\phi)$ [100].

Instead of implementing the numerical procedure elucidated in Ref. [74], we directly solve the background fields from Eqs. (5), (6), and (7). To simplify the computation, Eq. (5) can be integrated into a first-order differential equation

$$f'+f_c\,\mathrm{e}^{-3A_E}z^3=0, \tag{17}$$

where f_c is the integral constant. In view of $\Delta=3$, the UV asymptotic forms of the background fields at $z\to 0$ can be obtained as

$$\begin{aligned}A_E(z)=&-\frac{2p_1^2}{27}z^2+\cdots,\\ f(z)=&1-\frac{f_c}{4}z^4+\cdots,\\ \phi(z)=&p_1z+p_3z^3+\frac{4p_1^3}{9}\left(12b_4-6\gamma^4+1\right)z^3\log z+\cdots,\end{aligned} \tag{18}$$

with three independent parameters p_1, p_3, and f_c. As we have $f(z_h)=0$, to guarantee the regular behavior of $\phi(z)$ near the horizon, Eq. (7) must satisfy a natural IR boundary condition at $z=z_h$,

$$\left[f'\phi'-\frac{3\mathrm{e}^{2A_E}}{8z^2}\partial_\phi V_E(\phi)\right]_{z=z_h}=0. \tag{19}$$

With the UV asymptotic form (18) and the IR boundary condition (19), the background fields f, A_E, and ϕ can be solved numerically from Eqs. (6), (7), and (17). We find that the dilaton potential (10) with $\gamma=0.55$, $b_2=0.315$, and $b_4=-0.125$ can efficiently reproduce the two-flavor lattice QCD results of the equation of state. Note that γ and b_2 are related by the formula (11). Parameter $p_1=0.675\,\mathrm{GeV}$ is also fitted by the lattice results, and the 5D Newton constant is taken as $G_5=1$ in our consideration. Parameters p_3 and f_c in (18) are constrained by the IR boundary condition (19), and thus, depend on horizon z_h or temperature T. We show the z_h-dependence of parameter f_c and temperature T in Fig. 1. Both f_c and T decrease monotonically towards zero with the increase of z_h, which implies that our black hole solution persists in the entire range of T. We also show parameter p_3 as a function of T in Fig. 2, where we see that p_3 varies very slowly in the range of $T=0\sim 0.2\,\mathrm{GeV}$, then decreases and approaches negative values at around $T\simeq 0.28\,\mathrm{GeV}$.

The temperature dependences of entropy density s/T^3 and speed of sound squared c_s^2 are shown in Fig. 3, while in Fig. 4 we compare the numerical results of pressure $3p/T^4$ and energy density ε/T^4 in units of T^4 with the lattice interpolation results for the B-mass ensemble considered in Ref. [100]. In Fig. 5, we present the model result of trace anomaly $(\varepsilon-3p)/T^4$, which is also compared with the lattice interpolation result. We see that the Ein-

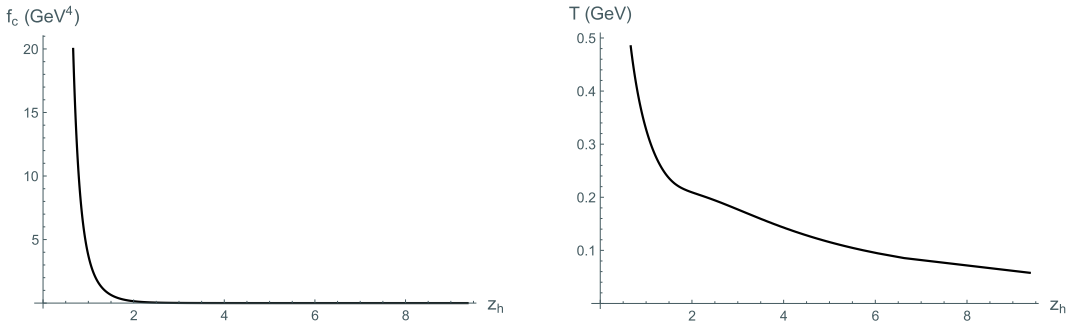

Fig. 1. z_h-dependence of parameter f_c and temperature T.

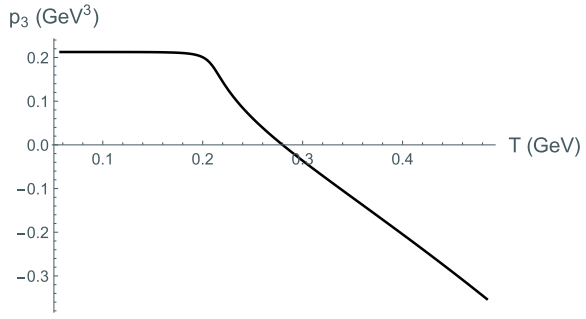

Fig. 2. Temperature dependence of parameter p_3.

stein-dilaton system with a nontrivial dilaton potential can generate crossover behavior of the equation of state, which matches well with the lattice results.

2.4 Polyakov loop

The deconfining phase transition in thermal QCD is characterized by the VEV of the Polyakov loop, which is defined as

$$L(T)=\frac{1}{N_c}\mathrm{tr}P\exp\left[\mathrm{i}g\int_0^{1/T}\mathrm{d}\tau\hat{A}_0\right], \tag{20}$$

where $\hat{A}_0$ is the time component of the non-Abelian gauge field operator, and symbol P denotes path ordering, and the trace is over the fundamental representation of $SU(N_c)$.

The VEV of the Polyakov loop in AdS/CFT is schematically given by the world-sheet path integral

$$\langle L\rangle=\int DX\mathrm{e}^{-S_w}, \tag{21}$$

where X is a set of world-sheet fields, and S_w is the classical world-sheet action [76, 77]. In principle, $\langle L\rangle$ can be evaluated approximately in terms of the minimal surface of the string world-sheet with given boundary conditions. In the low-energy and large N_c limit, we have $\langle L\rangle\sim\mathrm{e}^{-S_{NG}}$ with the Nambu-Goto action

$$S_{NG}=\frac{1}{2\pi\alpha'}\int\mathrm{d}^2\sigma\sqrt{\det(g^S_{\mu\nu}\partial_aX^\mu\partial_bX^\nu)}, \tag{22}$$

where α' denotes the string tension, $g^S_{\mu\nu}$ is the string-frame metric, and $X^\mu=X^\mu(\tau,\sigma)$ is the embedding of the world-sheet in the bulk spacetime. The regularized minimal world-sheet area takes the form

$$S_R=\frac{g_p}{\pi T}\int_\epsilon^{z_h}\mathrm{d}z\frac{\mathrm{e}^{2A_s}}{z^2}, \tag{23}$$

with $g_p=\dfrac{L^2}{2\alpha'}$ [76]. Subtracting the UV divergent terms and letting $\epsilon\to0$, the renormalized world-sheet area can be obtained as

$$\begin{aligned}S_0=&S_0'+c_p=\frac{g_p}{\pi T}\int_0^{z_h}\mathrm{d}z\left[\frac{\mathrm{e}^{2A_s}}{z^2}-\left(\frac{1}{z^2}+\frac{4p_1}{3z}\right)\right]\\&+\frac{g_p}{\pi T}\left(\frac{4p_1}{3}\log z_h-\frac{1}{z_h}\right)+c_p,\end{aligned} \tag{24}$$

where c_p is a scheme-dependent normalization constant. Thus the VEV of the Polyakov loop can be written as

$$\langle L\rangle=w\mathrm{e}^{-S_0}=\mathrm{e}^{-S_0'+c_p'}, \tag{25}$$

where w is a weight coefficient and the normalization constant $c_p'=\ln w-c_p$.

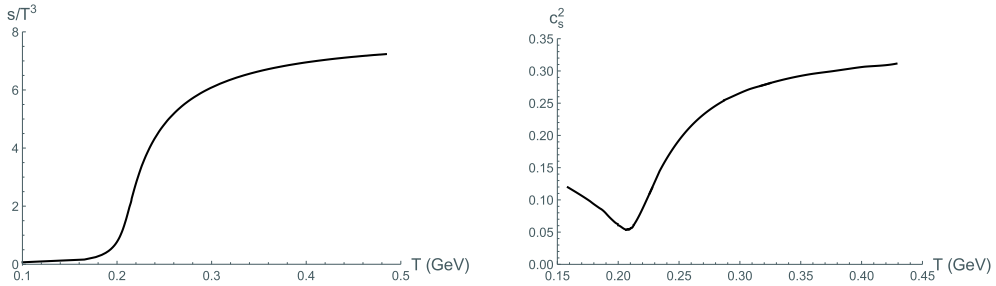

Fig. 3. Model results of entropy density s/T^3 (left panel) and speed of sound squared c_s^2 (right panel) as functions of T obtained from the Einstein-dilaton system.

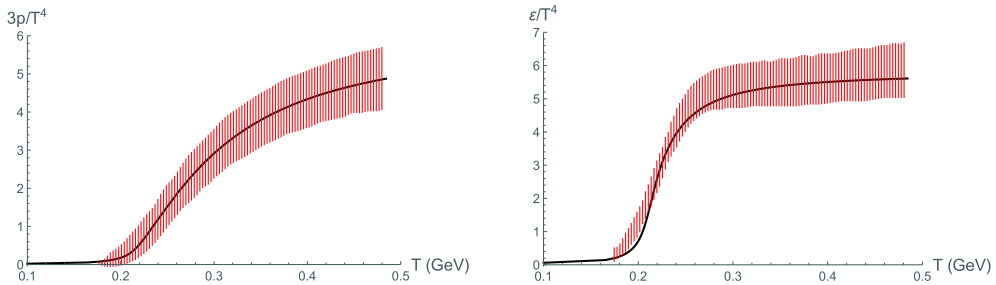

Fig. 4. (color online) Model results of pressure $3p/T^4$ (left panel) and energy density ε/T^4 (right panel) as functions of T compared with the lattice interpolation results of the two-flavor QCD, depicted by the red band [100].

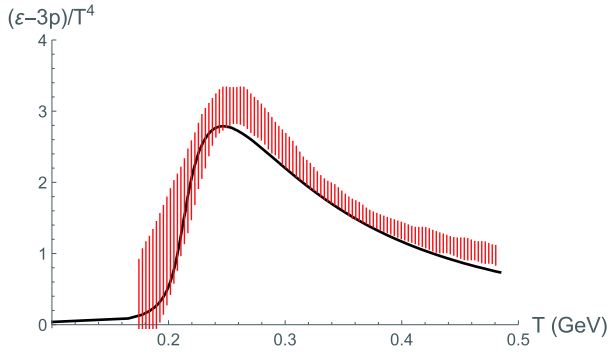

Fig. 5. (color online) Model result of trace anomaly $(\varepsilon-3p)/T^4$ as a function of T compared with the lattice interpolation results of the two-flavor QCD depicted by the red band [100].

We plot the temperature-dependent behavior of $\langle L\rangle$ with the parameter values $g_p = 0.29$ and $c_p' = 0.16$ in Fig. 6, where we also show the two-flavor lattice data of the renormalized Polyakov loop (corresponding to the B-mass ensemble in [100]). We can see that the model result fits the lattice data quite well when we choose proper values of g_p and c_p'.

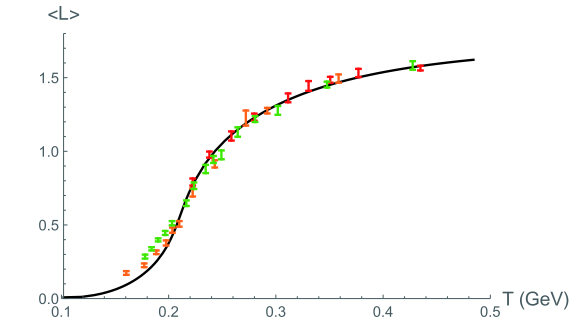

Fig. 6. (color online) Model result of the VEV of Polyakov loop $\langle L\rangle$ as a function of T compared with lattice data of renormalized Polyakov loop for the B-mass ensemble denoted by the colored points with error bars [100].

2.5 On the stability of the black hole solution

One remark must be made on the background solution of the Einstein-dilaton system. In the above description of the equation of state, we have only used the black hole solution, which is asymptotic to AdS_5 near the boundary; further, we have seen that this is crucial for the realization of the crossover transition. However, in principle, the Einstein-dilaton system also admits a thermal gas solution, which can be obtained by setting $f(z) = 1$ [49, 72]. To guarantee the soundness of our calculation, we must verify the stability of the black hole solution against the thermal gas one.

According to AdS/CFT, the free energy is related to the on-shell action of the background fields by $\beta\mathcal{F} = \mathcal{S}^R$ with $\beta = 1/T$, and the regularized on-shell action consists of three parts:

$$\mathcal{S}^R = \mathcal{S}_E + \mathcal{S}_{\rm GH} + \mathcal{S}_{\rm count} = \mathcal{S}_\epsilon + \mathcal{S}_{\rm IR} + \mathcal{S}_{\rm count}, \tag{26}$$

where $\mathcal{S}_E$ denotes the on-shell Einstein-Hilbert action, $\mathcal{S}_{\rm GH}$ denotes the Gibbons-Hawking term, and $\mathcal{S}_{\rm count}$ denotes the counter term. Subscripts ϵ and IR denote the contributions at UV cut-off $z = \epsilon$ and IR cut-off $z = z_{\rm IR}$, respectively. Following Ref. [49], we can obtain the regularized on-shell action of the black hole (BH) solution:

$$\mathcal{S}_{\rm BH} = \mathcal{S}^\epsilon_{\rm BH} + \mathcal{S}^{\rm count}_{\rm BH} = 2\beta M^3 V_3\Big(3b^2(\epsilon)f(\epsilon)b'(\epsilon) + \frac{1}{2}b^3(\epsilon)f'(\epsilon)\Big) + \mathcal{S}^{\rm count}_{\rm BH}, \tag{27}$$

where $M^3 \equiv 1/(16\pi G_5)$, V_3 is the three-space volume, and $b(z) \equiv \frac{L}{z}e^{A_E(z)}$. Note that $\mathcal{S}_{\rm BH}$ has no IR contribution due to $f(z_h) = 0$. The regularized on-shell action of the thermal gas (TG) solution takes the form:

$$\mathcal{S}_{\rm TG} = \mathcal{S}^\epsilon_{\rm TG} + \mathcal{S}^{\rm IR}_{\rm TG} + \mathcal{S}^{\rm count}_{\rm TG} = 2\tilde\beta \tilde M^3 \tilde V_3\big(3b_0^2(\epsilon)b_0'(\epsilon) + b_0^2(z_{\rm IR})b_0'(z_{\rm IR})\big) + \mathcal{S}^{\rm count}_{\rm TG}, \tag{28}$$

where $b_0(z) \equiv \frac{L}{z}e^{A_{E0}(z)}$ and $\tilde\beta, \tilde V_3$ denote the corresponding quantities in the thermal gas case. To compare the free energies, we must make sure that the intrinsic geometries near the boundary are the same for the two background solutions, i.e., the proper length of time circle and proper volume of three-space should be the same at $z = \epsilon$, which imposes the following conditions [49]:

$$\tilde\beta b_0(\epsilon) = \beta b(\epsilon)\sqrt{f(\epsilon)}, \quad \tilde V_3 b_0^3(\epsilon) = V_3 b^3(\epsilon). \tag{29}$$

With the condition (29), the free energy difference between the two background solutions has the form:

$$\mathcal{F} = \beta^{-1}\lim_{\epsilon\to 0}(\mathcal{S}_{\rm BH} - \mathcal{S}_{\rm TG}) = 2M^3V_3\Big(3b^2(\epsilon)f(\epsilon)b'(\epsilon) + \frac{1}{2}b^3(\epsilon)f'(\epsilon) - 3\frac{b^4(\epsilon)}{b_0^2(\epsilon)}\sqrt{f(\epsilon)}b_0'(\epsilon)\Big), \tag{30}$$

where the IR contribution in (28) has been omitted, as this term vanishes for good singularities [49]. In terms of the UV asymptotic forms (18), we obtain the following result:

$$\mathcal{F} = -\frac{1}{4}f_c L^3 M^3 V_3, \tag{31}$$

where we have taken the limit $\epsilon \to 0$. Note that the UV divergent terms in $\mathcal{S}_{\rm BH}$ and $\mathcal{S}_{\rm TG}$ have the same form, thus cancelling in the final result. As $f_c > 0$, we have $\mathcal{F} < 0$, which implies that the black hole phase is more stable than the thermal gas phase.

3 Chiral transition in improved soft-wall model with solved background

Our previous studies have shown that the chiral trans-

ition at zero baryon chemical potential can be characterized by an improved soft-wall AdS/QCD model in the AdS-Schwarzschild black hole background [93, 96]. However, this black hole solution cannot describe the QCD equation of state due to the conformal invariance of the dual gauge theory. The main aim of this work is to combine the advantages of the improved soft-wall model in the description of chiral transition with a background system that can reproduce the deconfinement properties of QCD. As a first attempt, we investigate the possible approaches to produce the chiral transition behaviors in the two-flavor case based on an improved soft-wall model (as the flavor part) under the more realistic background solved from the above Einstein-dilaton system.

3.1 Flavor action

We first outline the improved soft-wall AdS/QCD model with two flavors, which is proposed in Ref. [93]. The bulk action relevant to the chiral transition in this model is the scalar sector,

$$S_X^{isw} = -\int \mathrm{d}^5x\sqrt{-g}\mathrm{e}^{-\Phi}\mathrm{Tr}\left\{|\partial X|^2 + V_X(X)\right\}, \tag{32}$$

where the dilaton takes the form $\Phi(z)=\mu_g^2 z^2$ to produce the linear Regge spectra of light mesons, and the scalar potential is

$$V_X(X) = m_5^2(z)|X|^2 + \lambda|X|^4, \tag{33}$$

with a running bulk mass $m_5^2(z) = -3-\mu_c^2 z^2$. The constant term of $m_5^2(z)$ is determined by the mass-dimension relation $m_5^2L^2=\Delta(\Delta-4)$ for a bulk scalar field [15, 16], while the z-squared term is motivated by the phenomenology of the meson spectrum and the quark mass anomalous dimension [93].

In the holographic framework, a natural mechanism to produce such a z-dependent term of $m_5^2(z)$ is to introduce a coupling between the dilaton and the bulk scalar field. As we can see, without changing the results of the improved soft-wall model, the scalar potential can be recast into another form

$$V_X(X,\Phi) = m_5^2|X|^2 - \lambda_1\Phi|X|^2 + \lambda_2|X|^4, \tag{34}$$

where $m_5^2=-3$, and a cubic coupling term of Φ and X has been introduced. The effects of similar couplings on the low-energy hadron properties have also been considered in previous studies [32]. Here, we propose such a change of V_X from (33) to (34) with the aim to describe the chiral transition behaviors for the two-flavor case. Thus, the flavor action that will be addressed in this work is

$$S_X = -\int \mathrm{d}^5x\sqrt{-g}\mathrm{e}^{-\Phi}\mathrm{Tr}\left\{|\partial X|^2 + V_X(X,\Phi)\right\}. \tag{35}$$

Unlike in previous studies, the metric and the dilaton in the flavor action (35) will be solved from the Einstein-dilaton system (6), (7), and (17), which has been shown to reproduce the two-flavor lattice results of the equation of state. We assume that the flavor action (35) has been written in the string frame with the metric ansatz (2). In our model, the dilaton field ϕ in the background action (1) has been distinguished from the field Φ in the flavor action (35). From AdS/CFT, these two fields may be reasonably identified as the same one, as indicated by the Dirac-Born-Infeld action, which dictates the dynamics of the open string sector with the string coupling $g_s=\mathrm{e}^{\phi}$. This is implemented in some studies [32]. However, the low-energy and large-N limits taken in AdS/CFT and the further reduction to AdS/QCD have made things more subtle. The exact correspondence between g_s and e^{ϕ} is not consolidated in the bottom-up AdS/QCD. In contrast, the dilaton term $\mathrm{e}^{-\Phi}$ in the flavor sector has been introduced to realize the Regge spectra of hadrons [18]. In this work, we concentrate on the phenomenological aspects and study how to realize more low-energy properties of QCD by the holographic approach. Thus, we attempt a more general form $\Phi=k\phi$ with k a parameter, which will not affect the linear Regge spectra qualitatively. In the actual calculation, we choose two simplest cases $k=1$ and $k=2$ to investigate the effects of k on chiral behaviors. The probe approximation that neglects the backreaction effect of the flavor sector on the background system is adopted in this work, as in most studies on AdS/QCD with a fixed background.

3.2 EOM of the scalar VEV

According to AdS/CFT, the VEV of the bulk scalar field in the two-flavor case can be written as $\langle X\rangle = \frac{\chi(z)}{2}I_2$ with I_2 denoting the 2×2 identity matrix, and the chiral condensate is incorporated in the UV expansion of the scalar VEV $\chi(z)$ [16]. To address the issue on chiral transition, we only need to consider the action of the scalar VEV,

$$S_\chi = -\int \mathrm{d}^5x\sqrt{-g}\mathrm{e}^{-\Phi}\left(\frac{1}{2}g^{zz}(\partial_z\chi)^2 + V(\chi,\Phi)\right), \tag{36}$$

with

$$V(\chi,\Phi) = \mathrm{Tr}\,V_X(\langle X\rangle,\Phi) = \frac{1}{2}(m_5^2-\lambda_1\Phi)\chi^2 + \frac{\lambda_2}{8}\chi^4. \tag{37}$$

In terms of the metric ansatz (2), the EOM of $\chi(z)$ can be derived from the action (36) as

$$\chi'' + \left(3A_S' - \Phi' + \frac{f'}{f} - \frac{3}{z}\right)\chi' - \frac{\mathrm{e}^{2A_S}\partial_\chi V(\chi,\Phi)}{z^2 f} = 0. \tag{38}$$

The UV asymptotic form of $\chi(z)$ at $z\to0$ can be obtained from Eq. (38) as

$$\begin{aligned}\chi(z) =& m_q\zeta z + (6-k+k\lambda_1)m_q p_1\zeta z^2 + \frac{\sigma}{\zeta}z^3 \\ &+ \frac{1}{3}\left[m_q\zeta p_1^2\left(30k-3k^2-23k\lambda_1-\frac{3}{2}k^2\lambda_1^2\right.\right. \\ &\left.\left.+\frac{9}{2}k^2\lambda_1-\frac{224}{3}\right)+\frac{3}{4}m_q^3\zeta^3\lambda_2\right]z^3\log z+\cdots,\end{aligned} \tag{39}$$

where m_q is the current quark mass, σ is the chiral condensate, and $\zeta = \frac{\sqrt{N_c}}{2\pi}$ is a normalization constant [20]. As in Eq. (7), a natural boundary condition at horizon z_h follows from the regular condition of $\chi(z)$ near z_h,

$$\left[f'\chi' - \frac{e^{2A_s}}{z^2}\partial_\chi V(\chi,\Phi)\right]_{z=z_h} = 0. \tag{40}$$

3.3 Chiral transition

To study the chiral transition properties in the improved soft-wall AdS/QCD model with the given background, we must solve the scalar VEV $\chi(z)$ numerically from Eq. (38) with the UV asymptotic form (39) and the IR boundary condition (40). The chiral condensate can then be extracted from the UV expansion of $\chi(z)$. In the calculation, we take the set of parameter values that has been used to fit the lattice results of the equation of state in the two-flavor case (see Sec. 2.3), and the quark mass is fixed as $m_q = 5$ MeV.

In this work, we only consider two cases corresponding to $k = 1$ ($\Phi = \phi$) and $k = 2$ ($\Phi = 2\phi$). In each case, the temperature dependence of the chiral condensate normalized by $\sigma_0 = \sigma(T = 0)$ is investigated for a set of values of λ_1 and λ_2. We first fix $\lambda_2 = 1$, and select four different values of λ_1 for each case. The model results of the normalized chiral condensate σ/σ_0 as a function of T are shown in Fig. 7. We can see that the crossover transition can be realized qualitatively in such an improved soft-wall model with the solved gravitational background. Moreover, we find that there is a decreasing tendency for the transition temperature with the decrease of λ_1, yet a visible bump emerges near the transition region at relatively smaller λ_1 and only disappears gradually with the increase of λ_1. As shown in Fig. 7, we find that the transition temperatures with our selected parameter values are larger than the lattice result $T_\chi \sim 193$ MeV [100].

We then investigate the effects of the quartic coupling constant λ_2 on chiral transitions. We fix $\lambda_1 = -1.4$ for the case $k = 1$ and $\lambda_1 = -0.5$ for the case $k = 2$, and select four different values of λ_2 in each case. The chiral transition curves are plotted in Fig. 8. The result shows that with the increase of λ_2 the bump near the transition region becomes smaller, and the normalized chiral condensate σ/σ_0 descends gently with T, though the value of λ_2 needs to be considerably large to smooth across the bump.

4 Conclusion and discussion

We considered an improved soft-wall AdS/QCD model with a cubic coupling term between the dilaton and the bulk scalar field in a more realistic background, which is solved from the Einstein-dilaton system with a nontrivial dilaton potential. Such an Einstein-dilaton system was used to reproduce the equation of state from lattice QCD with two flavors. Then, the chiral transition behaviors were investigated in the improved soft-wall model based on the solved bulk background. We only considered two typical cases with $k = 1$ and $k = 2$, and the

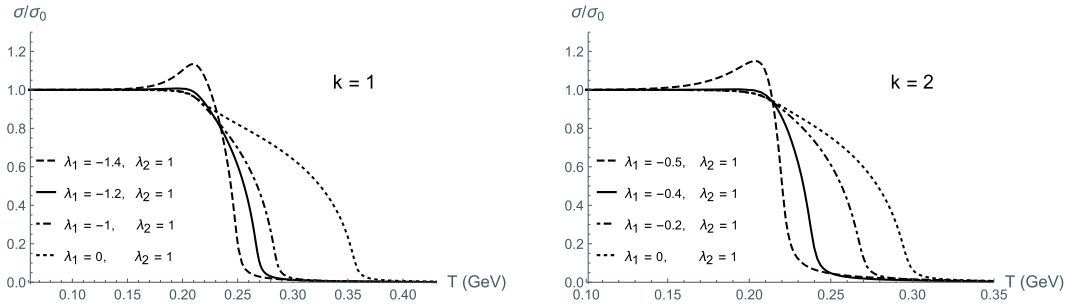

Fig. 7. Normalized chiral condensate σ/σ_0 as a function of T for different values of λ_1 in cases $k = 1$ and $k = 2$ with $\lambda_2 = 1$.

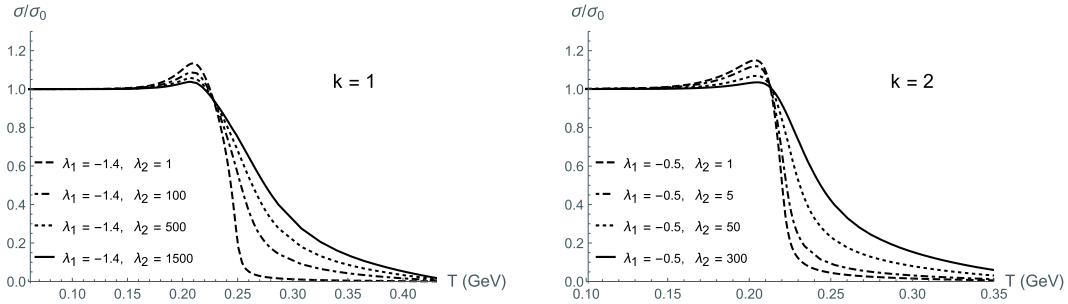

Fig. 8. Normalized chiral condensate σ/σ_0 as a function of T for different values of λ_2 in cases $k = 1$ and $k = 2$ with fixed values of λ_1.

quartic coupling constant is first fixed as $\lambda_2 = 1$. In both cases, the crossover behavior of chiral transition can be realized, as seen from Fig. 7. Nevertheless, the chiral transition temperatures obtained from the model are significantly larger than the lattice result. Although T_χ decreases with the decrease in λ_1, a visible bump near the transition region emerges when λ_1 is small enough. We then studied the influence of the value of λ_2 on the chiral transition, as shown in Fig. 8. We find that in some sense, the quartic coupling term can smooth the bump; however, to remove it, the value of λ_2 must be considerably large.

In our consideration, the scaling dimension of the dual operator $\mathrm{tr}\,F_{\mu\nu}^2$ of the dilaton has been taken as $\Delta = 3$, which can be used to mimick the QCD equation of state [78, 79]. However, we remark that the properties of thermal QCD considered in our work are not determined exclusively by one particular value of Δ. Indeed, other values of Δ have also been adopted for the realization of the equation of state with slightly different forms of $V_E(\phi)$ [73, 77]. Because the UV matching to QCD at a finite scale cannot capture asymptotic freedom, we are content to provide a phenomenological description on the thermodynamic properties of QCD, which are expected not to be so sensitive to the UV regime from the angle of renormalization and effective field theory. In this study, we have built an improved soft-wall AdS/QCD model under a more realistic gravitational background, which provides a possibility in the holographic framework to address the deconfining and chiral phase transition simultaneously.

We have assumed that the backreaction of the flavor sector to the background is sufficiently small, such that we can adopt the solution of the Einstein-dilaton system as the bulk background, under which the chiral properties of the improved soft-wall model are considered. This is sensible only when we take a small weight of the flavor action (35) compared to the background action (1). To clarify the phase structure in this improved soft-wall AdS/QCD model, we must thoroughly consider the backreaction of the flavor part to the background system. The correlation between the deconfining and chiral phase transitions can then be studied with such an improved soft-wall model coupled with an Einstein-dilaton system. The case of finite chemical potential can also be considered by introducing a $U(1)$ gauge field to study the properties of the QCD phase diagram.

References

1 M. A. Stephanov, *Proceedings*, *24th International Symposium on Lattice Field Theory* (Lattice 2006): Tucson, USA, July 23-28, 2006, PoS LAT2006, 024 (2006), arXiv: hep-lat/0701002 [hep-lat]
2 Y. Aoki, G. Endrodi, Z. Fodor *et al*., Nature, **443**: 675 (2006), arXiv:hep-lat/0611014[hep-lat]
3 A. Bazavov *et al*., Phys. Rev. D, **85**: 054503 (2012), arXiv:1111.1710[hep-lat]
4 T. Bhattacharya *et al*., Phys. Rev. Lett., **113**: 082001 (2014), arXiv:1402.5175[hep-lat]
5 C. D. Roberts and S. M. Schmidt, Prog. Part. Nucl. Phys., **45**: S1 (2000), arXiv:nuclth/0005064[nucl-th]
6 J. Braun and H. Gies, JHEP, **06**: 024 (2006), arXiv:hep-ph/0602226[hep-ph]
7 C. S. Fischer, Phys. Rev. Lett., **103**: 052003 (2009), arXiv:0904.2700[hep-ph]
8 K. Fukushima, Phys. Lett. B, **591**: 277 (2004), arXiv:hep-ph/0310121[hep-ph]
9 J. M. Maldacena, Int. J. Theor. Phys., **38**: 1113 (1999), arXiv:hep-th/9711200[hep-th]
10 S. S. Gubser, I. R. Klebanov, and A. M. Polyakov, Phys. Lett. B, **428**: 105 (1998), arXiv:hepth/9802109[hep-th]
11 E. Witten, Adv. Theor. Math. Phys., **2**: 253 (1998), arXiv:hep-th/9802150[hep-th]
12 M. Kruczenski, D. Mateos, R. C. Myers *et al*., JHEP, **05**: 041 (2004), arXiv:hepth/0311270[hep-th]
13 T. Sakai and S. Sugimoto, Prog. Theor. Phys., **113**: 843 (2005), arXiv:hep-th/0412141[hep-th]
14 T. Sakai and S. Sugimoto, Prog. Theor. Phys., **114**: 1083 (2005), arXiv:hep-th/0507073[hepth]
15 L. Da Rold and A. Pomarol, Nucl. Phys. B, **721**: 79 (2005), arXiv:hep-ph/0501218[hep-ph]
16 J. Erlich, E. Katz, D. T. Son *et al*., Phys. Rev. Lett., **95**: 261602 (2005), arXiv:hep-ph/0501128[hep-ph]
17 G. F. de Teramond and S. J. Brodsky, Phys. Rev. Lett., **94**: 201601 (2005), arXiv:hepth/0501022[hep-th]
18 A. Karch, E. Katz, D. T. Son *et al*., Phys. Rev. D, **74**: 015005 (2006), arXiv:hep-ph/0602229[hep-ph]
19 C. Csaki and M. Reece, JHEP, **05**: 062 (2007), arXiv:hep-ph/0608266[hep-ph]
20 A. Cherman, T. D. Cohen, and E. S. Werbos, Phys. Rev. C, **79**: 045203 (2009), arXiv:0804.1096[hep-ph]
21 T. Gherghetta, J. I. Kapusta, and T. M. Kelley, Phys. Rev. D, **79**: 076003 (2009), arXiv:0902.1998[hep-ph]
22 T. M. Kelley, S. P. Bartz, and J. I. Kapusta, Phys. Rev. D, **83**: 016002 (2011), arXiv:1009.3009 [hep-ph]
23 Y.-Q. Sui, Y.-L. Wu, Z.-F. Xie *et al*., Phys. Rev. D, **81**: 014024 (2010), arXiv:0909.3887[hep-ph]
24 Y.-Q. Sui, Y.-L. Wu, and Y.-B. Yang, Phys. Rev. D, **83**: 065030 (2011), arXiv:1012.3518 [hep-ph]
25 M. Fujita, K. Fukushima, T. Misumi *et al*., Phys. Rev. D, **80**: 035001 (2009), arXiv:0903.2316[hep-ph]
26 M. Fujita, T. Kikuchi, K. Fukushima *et al*., Phys. Rev. D, **81**: 065024 (2010), arXiv:0911.2298[hep-ph]
27 P. Colangelo, F. Giannuzzi, and S. Nicotri, Phys. Rev. D, **80**: 094019 (2009), arXiv:0909.1534 [hep-ph]
28 P. Colangelo, F. Giannuzzi, S. Nicotri *et al*., Eur. Phys. J. C, **72**: 2096 (2012), arXiv:1112.4402[hep-ph]
29 L.-X. Cui, Z. Fang, and Y.-L. Wu, Eur. Phys. J. C, **76**: 22 (2016), arXiv:1310.6487[hep-ph]
30 L.-X. Cui, Z. Fang, and Y.-L. Wu, Chin. Phys. C, **40**: 063101 (2016), arXiv:1404.0761[hep-ph]
31 D. Li, M. Huang, and Q.-S. Yan, Eur. Phys. J. C, **73**: 2615 (2013), arXiv:1206.2824[hep-th]
32 D. Li and M. Huang, JHEP, **11**: 088 (2013), arXiv:1303.6929[hep-ph]
33 E. V. Shuryak, *Quark gluon plasma. New discoveries at RHIC: A case of strongly interacting quark gluon plasma*. Proceedings, RBRC Workshop, Brookhaven, Upton, USA, May 14-15, 2004, Nucl. Phys. A,750, 64 (2005), arXiv: hep-ph/0405066 [hep-ph]
34 S. J. Brodsky, G. F. de Teramond, H. G. Dosch *et al*., Phys. Rept., **584**: 1 (2015), arXiv:1407.8131[hep-ph]
35 M. J. Tannenbaum, Rept. Prog. Phys., **69**: 2005 (2006), arXiv:nucl-ex/0603003[nucl-ex]

36 G. Policastro, D. T. Son, and A. O. Starinets, Phys. Rev. Lett., **87**: 081601 (2001), arXiv:hepth/0104066[hep-th]
37 R.-G. Cai, Z.-Y. Nie, N. Ohta *et al*., Phys. Rev. D, **79**: 066004 (2009), arXiv:0901.1421[hep-th]
38 R.-G. Cai, Z.-Y. Nie, and Y.-W. Sun, Phys. Rev. D, **78**: 126007 (2008), arXiv:0811.1665 [hep-th]
39 S.-J. Sin and I. Zahed, Phys. Lett. B, **608**: 265 (2005), arXiv:hep-th/0407215[hep-th]
40 E. Shuryak, S.-J. Sin, and I. Zahed, J. Korean Phys. Soc., **50**: 384 (2007), arXiv:hepth/0511199[hep-th]
41 H. Nastase, (2005), arXiv: hep-th/0501068[hep-th]
42 S. Nakamura and S.-J. Sin, JHEP, **09**: 020 (2006), arXiv:hep-th/0607123[hep-th]
43 S.-J. Sin, S. Nakamura, and S. P. Kim, JHEP, **12**: 075 (2006), arXiv:hep-th/0610113[hep-th]
44 R. A. Janik and R. B. Peschanski, Phys. Rev. D, **73**: 045013 (2006), arXiv:hep-th/0512162 [hep-th]
45 C. P. Herzog, A. Karch, P. Kovtun *et al*., JHEP, **07**: 013 (2006), arXiv:hep-th/0605158[hep-th]
46 U. Gursoy and E. Kiritsis, JHEP, **02**: 032 (2008), arXiv:0707.1324[hep-th]
47 U. Gursoy, E. Kiritsis, and F. Nitti, JHEP, **02**: 019 (2008), arXiv:0707.1349[hep-th]
48 U. Gursoy, E. Kiritsis, L. Mazzanti *et al*., Phys. Rev. Lett., **101**: 181601 (2008), arXiv:0804.0899[hep-th]
49 U. Gursoy, E. Kiritsis, L. Mazzanti *et al*., JHEP, **05**: 033 (2009), arXiv:0812.0792 [hep-th]
50 D. Li, J. Liao, and M. Huang, Phys. Rev. D, **89**: 126006 (2014), arXiv:1401.2035[hep-ph]
51 D. Li, S. He, and M. Huang, JHEP, **06**: 046 (2015), arXiv:1411.5332[hep-ph]
52 Z. Fang, D. Li, and Y.-L. Wu, Phys. Lett. B, **754**: 343 (2016), arXiv:1602.00379[hep-ph]
53 Z. Fang, Phys. Rev. D, **94**: 074017 (2016), arXiv:1607.06197[hep-ph]
54 Z. Fang, Phys. Lett. B, **758**: 1 (2016)
55 N. Evans, C. Miller, and M. Scott, Phys. Rev. D, **94**: 074034 (2016), arXiv:1604.06307[hepph]
56 K. A. Mamo, Phys. Rev. D, **94**: 041901 (2016), arXiv:1606.01598[hep-th]
57 D. Dudal and S. Mahapatra, JHEP, **04**: 031 (2017), arXiv:1612.06248[hep-th]
58 D. Dudal and T. G. Mertens, Phys. Rev. D, **97**: 054035 (2018), arXiv:1802.02805[hep-th]
59 A. Ballon-Bayona, M. Ihl, J. P. Shock *et al*., JHEP, **10**: 038 (2017), arXiv:1706.05977 [hep-th]
60 J. Chen, S. He, M. Huang *et al*., JHEP, **01**: 165 (2019), arXiv:1810.07019[hep-ph]
61 M. Attems, J. Casalderrey-Solana, D. Mateos *et al*., JHEP, **10**: 155 (2016), arXiv:1603.01254[hep-th]
62 M. Attems, J. Casalderrey-Solana, D. Mateos *et al*., JHEP, **06**: 154 (2017), arXiv:1703.09681[hep-th]
63 S. S. Gubser, (1999), arXiv: hep-th/9902155[hep-th]
64 I. H. Brevik, K. Ghoroku, and A. Nakamura, Int. J. Mod. Phys. D, **15**: 57 (2006), arXiv:hepth/0505057[hep-th]
65 A. Karch and E. Katz, JHEP, **06**: 043 (2002), arXiv:hep-th/0205236[hep-th]
66 M. Kruczenski, D. Mateos, R. C. Myers *et al*., JHEP, **07**: 049 (2003), arXiv:hepth/0304032[hep-th]
67 J. Erdmenger, N. Evans, I. Kirsch *et al*., Eur. Phys. J. A, **35**: 81 (2008), arXiv:0711.4467[hep-th]
68 J. Babington, J. Erdmenger, N. J. Evans *et al*., Phys. Rev. D, **69**: 066007 (2004), arXiv:hep-th/0306018[hep-th]
69 K. Ghoroku and M. Yahiro, Phys. Lett. B, **604**: 235 (2004), arXiv:hep-th/0408040[hep-th]
70 S. W. Hawking and D. N. Page, Commun. Math. Phys., **87**: 577 (1983)
71 E. Witten, Adv. Theor. Math. Phys., **2**: 505 (1998), arXiv:hep-th/9803131[hepth]
72 C. P. Herzog, Phys. Rev. Lett., **98**: 091601 (2007), arXiv:hep-th/0608151[hep-th]
73 S. S. Gubser, A. Nellore, S. S. Pufu *et al*., Phys. Rev. Lett., **101**: 131601 (2008), arXiv:0804.1950[hep-th]
74 S. S. Gubser and A. Nellore, Phys. Rev. D, **78**: 086007 (2008), arXiv:0804.0434[hep-th]
75 S. S. Gubser, S. S. Pufu, and F. D. Rocha, JHEP, **08**: 085 (2008), arXiv:0806.0407[hep-th]
76 O. Andreev, Phys. Rev. Lett., **102**: 212001 (2009), arXiv:0903.4375[hep-ph]
77 J. Noronha, Phys. Rev. D, **81**: 045011 (2010), arXiv:0910.1261[hep-th]
78 S. I. Finazzo and J. Noronha, Phys. Rev. D, **89**: 106008 (2014), arXiv:1311.6675[hep-th]
79 S. I. Finazzo and J. Noronha, Phys. Rev. D, **90**: 115028 (2014), arXiv:1411.4330[hep-th]
80 R. Yaresko and B. Kampfer, Phys. Lett. B, **747**: 36 (2015), arXiv:1306.0214[hep-ph]
81 R. Yaresko, J. Knaute, and B. Kämpfer, Eur. Phys. J. C, **75**: 295 (2015), arXiv:1503.09065 [hep-ph]
82 P. Colangelo, F. Giannuzzi, and S. Nicotri, Phys. Rev. D, **83**: 035015 (2011), arXiv:1008.3116 [hep-ph]
83 D. Li, S. He, M. Huang *et al*., JHEP, **09**: 041 (2011), arXiv:1103.5389[hep-th]
84 S. He, S.-Y. Wu, Y. Yang *et al*., JHEP, **04**: 093 (2013), arXiv:1301.0385[hep-th]
85 Y. Yang and P.-H. Yuan, JHEP, **11**: 149 (2014), arXiv:1406.1865[hep-th]
86 Z. Fang, S. He, and D. Li, Nucl. Phys. B, **907**: 187 (2016), arXiv:1512.04062[hep-ph]
87 R. Rougemont, R. Critelli, J. Noronha-Hostler *et al*., Phys. Rev. D, **96**: 014032 (2017), arXiv:1704.05558[hep-ph]
88 Z. Li, Y. Chen, D. Li *et al*., Chin. Phys. C, **42**: 013103 (2018), arXiv:1706.02238[hep-ph]
89 R. Zöllner and B. Kämpfer, (2018), arXiv: 1807.04260[hep-th]
90 X. Chen, D. Li, and M. Huang, Chin. Phys. C, **43**: 023105 (2019), arXiv:1810.02136[hep-ph]
91 K. Chelabi, Z. Fang, M. Huang *et al*., JHEP, **04**: 036 (2016), arXiv:1512.06493 [hep-ph]
92 K. Chelabi, Z. Fang, M. Huang *et al*., Phys. Rev. D, **93**: 101901 (2016), arXiv:1511.02721[hep-ph]
93 Z. Fang, Y.-L. Wu, and L. Zhang, Phys. Lett. B, **762**: 86 (2016), arXiv:1604.02571[hep-ph]
94 D. Li and M. Huang, JHEP, **02**: 042 (2017), arXiv:1610.09814[hep-ph]
95 S. P. Bartz and T. Jacobson, Phys. Rev. C, **97**: 044908 (2018), arXiv:1801.00358[hep-ph]
96 Z. Fang, Y.-L. Wu, and L. Zhang, Phys. Rev. D, **98**: 114003 (2018), arXiv:1805.05019[hep-ph]
97 S. P. Bartz and T. Jacobson, Phys. Rev. D, **94**: 075022 (2016), arXiv:1607.05751[hep-ph]
98 Z. Fang, Y.-L. Wu, and L. Zhang, Phys. Rev. D, **99**: 034028 (2019), arXiv:1810.12525[hep-ph]
99 Z. Fang, Y.-L. Wu, and L. Zhang, Phys. Rev. D, **100**: 054008 (2019), arXiv:1904.04695[hepph]
100 F. Burger, E.-M. Ilgenfritz, M. P. Lombardo *et al*., Phys. Rev. D, **91**: 074504 (2015), arXiv:1412.6748[hep-lat]